

Fabrication and Photoelectric Properties of Large Area ZnO Nanorod with Au Nanospheres

Chun-Li Luo¹ · Wei-Guo Yan² · Jianhua Han³ · Weiben Chen² · Jian Zhao¹ · Xin Wei⁴ · Jiwei Qi⁴ · Zhifeng Liu³

Received: 30 March 2015 / Accepted: 30 June 2015 / Published online: 24 July 2015
© Springer Science+Business Media New York 2015

Abstract Novel gold nanospheres top-contact ZnO nanorods arrays were fabricated via combination of self-assemble nanosphere lithography and low-cost hydrothermal chemical method. Gold nanoparticles of different geometries are used to enhance the fluorescent properties of ZnO nanorods based on localized surface plasmonic resonances. The results show that defect-related emission intensity ratio of the ZnO nanorods arrays can be improved up to two orders, and the defect-related emission peak red-shifted from 577 to 623 nm. This improvement is attributed to the enhanced localized surface plasmonic absorption of gold nanoparticles, which implies a promising application in surface plasmonic enhanced spectra.

Keywords Self-assemble · Surface plasmon · Nanostructure · ZnO nanorods · Gold nanosphere

Introduction

ZnO nanorods (NRs), as a low-cost, multifunctional, and environmental material, had received ongoing attention and wide applications in optoelectronics devices and light-emitting diode for several decades [1–3]. Nevertheless, the absorption band of ZnO NRs is limited to UV region due to their wide band gap and large exciton binding energy. In addition, another important factor is a large number of carriers' recombination, which resulted in low fluorescence efficiency. Therefore, considerable efforts have been made to enlarge the absorption spectrum in UV region to enhance fluorescence efficiency of ZnO NRs [4–10].

It is well-known that noble metal nanoparticles (NPs) support localized surface plasmonic resonances (LSPRs), which can effectively enhance utilization ratio of the light. Hence, some works focused on enhancing the fluorescence efficiency of ZnO nanostructures by using different metal particles (Ag, Au, Al, Cu, and Pt) as capping layers [11–15]. For example, H. D. Sun's group used gold NPs-capped ZnO NRs to efficiently enhance the band edge emission and suppress the defect-related emission [11]. The physical mechanism is that electrons in the defect states are pumped to the conduction band of ZnO by Au nanoparticles, and photons into free space will be suppressed due to non-radiative dissipation of the surface plasmon.

For metal NPs, their plasmonic absorption band is usually located in the visible and near-infrared region and can be effectively tuned by the NPs size and shape [16–18]. However, there is a strong absorption edge in UV region for ZnO nanorods. It is obvious that there is a difference between the two energy bands. Therefore, the resonance energy of metal NPs is very difficult to improve the ZnO band edge emission. However, ZnO NRs have other emission due to defects or impurities of ZnO, which is consistent with

✉ Wei-Guo Yan
yanweiguo@tcu.edu.cn

✉ Zhifeng Liu
tjulzf@163.com

¹ School of Control and Mechanical Engineering, Tianjin Chengjian University, Tianjin 300384, China

² School of Science, Tianjin Chengjian University, Tianjin 300384, China

³ School of Materials Science and Engineering, Tianjin Chengjian University, Tianjin 300384, China

⁴ Key Laboratory of Weak-Light Nonlinear Photonics, Ministry of Education, Teda Applied Physics School and School of Physics, Nankai University, Tianjin 300457, China

LSPRs of metal NPs. To the best knowledge, there are few reports about metal NPs served as an auxiliary layer, which is used to enhance defect-related luminescence of ZnO NRs.

In this study, the novel gold nanospheres (NSs) top-contact ZnO NRs were fabricated based on a combination of NS lithography (NSL) and thermal decomposed polymer method. Fluorescence properties of the bare and gold-capped ZnO NRs are studied. It is found that the defect emission of ZnO NRs can be obviously enhanced by top-contact Au NSs. The intensity ratio of the defect-related emission to the band gap emission can be improved up to 10 decades. At the same time, the defect-related emission peak red-shifted from 577 to 623 nm. The coupling mechanism between the Au NSs and ZnO NR arrays will be discussed in detail.

Experimental Section

Preparation of ZnO NRs

The synthesis of large size disorder ZnO NRs involves substrate pretreatment and hydrothermal growth [19, 20]. Firstly, indium tin oxide (ITO) substrates were cleaned for 0.5 h in acetone, isopropyl alcohol, and absolute ethanol in sequence by ultrasonic cleaner. Then, a seed layer was deposited onto an ITO glass by a sol-gel and dip-coating method. Next, the ZnO NRs were annealed at 400 °C in air for 1 h, followed by incubation in a mixed solution of 0.05 M zinc nitrate and 0.05 M hexamethylenetetramine (HMTA) at 90 °C for 4 h. The obtained samples were subsequently washed with distilled water and finally dried in air.

Fabrication of Au NSs Top-contacted ZnO NRs

The preparation of Au NSs top-contacted ZnO NRs involves three processes: firstly, the monolayer polystyrene spheres (PS) arrays with different diameters self-assembled on ZnO NRs by interface-transferred method [21]. Then, a 20-nm Au film was deposited on PS templates by electron beam deposition (EBD). Due to the limitation of the PS template, most Au particles attached to PS spheres surface and formed Au @PS arrays. Finally, ZnO NRs attached Au NSs structures formed when the samples annealed in the muffle furnace for 1 h at 300, 400, and 500 °C, respectively. The schematic illustration of the process is depicted in Fig. 1.

Characterization

The morphology and composition of the samples were investigated using a field-emission scanning electron microscopy (SEM) with an energy dispersive spectrometer (EDS) detector and transmission electron microscope (TEM). X-ray diffraction (XRD) was used for analysis of the crystal

structures. Photoluminescence (PL) measurements were performed by excitation from a 325 nm line of a continuous-wave He–Cd laser.

Results and Discussion

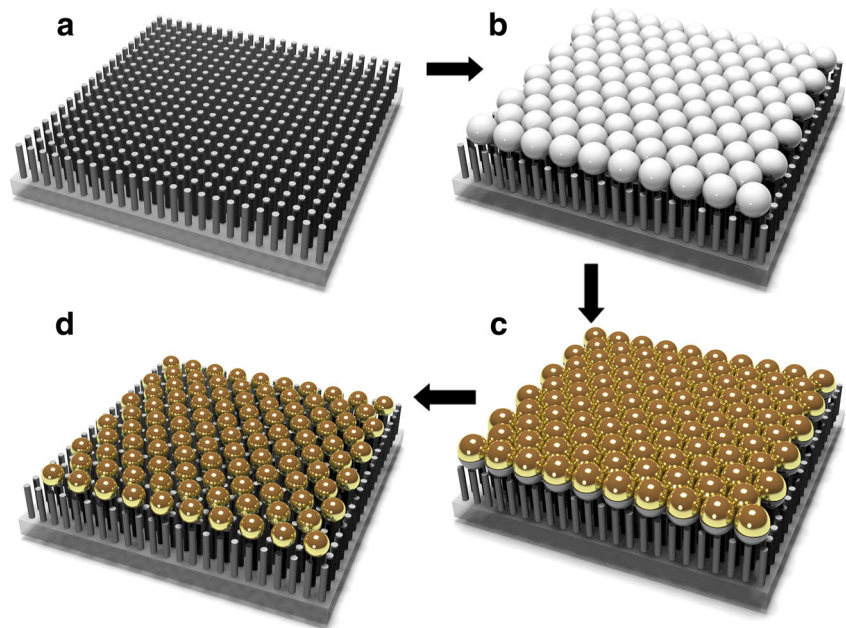
Fabrication of the Bare ZnO NRs and Au NSs Top-contacted ZnO NRs

Figure 2a shows the SEM images of ZnO NRs arrays with uniform alignment. The density and diameter of ZnO NRs are uniform distribution, and the diameter of ZnO NRs is about 100 nm. The interface-transferred method is used to prepare monolayer PS spheres arrays on ZnO NRs surface in the experiment. The hexagonal symmetry PS spheres arrays arranged onto ZnO NRs arrays, as is shown in Fig. 2b. At the same time, ZnO NRs structures can be observed clearly through the inter-space of the PS. Here, the diameter of PS sphere is 1000 nm. When a 20-nm Au film was deposited on ZnO NRs through the interstice of the PS. PS templates act as intermediate layers to form Au nanostructures on the top of ZnO NRs. The SEM images of Fig. 2c and d are that PS spheres arrays coated with 20-nm Au film annealed at 300 and 500 °C, respectively. When the sample annealed at 300 °C, the PS polymer decomposed and this temperature did not affect Au film coated on PS sphere. So, Au shell arrays formed on the ZnO NRs surface in Fig. 2c. While the annealing temperature increases to 500 °C, the Au film coated on PS templates formed Au NSs. Because of removing the PS cores, Au film on PS templates becomes unstable and yields Au NSs at higher temperature [22]. These Au NSs appeared random distribution due to the rough surface of ZnO NRs, as displayed in Fig. 2d. The formation of Au NSs is that few Au nanoparticles on ZnO NRs through the interstitial region of the PS arrays during the deposition of Au film act as Au seeds. With increasing of annealing temperature, Au seeds grow up Au NSs on the ZnO NRs.

Fabrication of Au NSs Top-contacted ZnO NRs with Different Density and Size

To compare the influence of the PS sphere size on ZnO NRs, PS sphere arrays with the size of 200, 500, 750, and 1000 nm were transferred on ZnO NRs, respectively, as is shown in Fig. 3a–d. We can see that PS sphere arrays with 200 nm diameter are unordered and overlap during the interface-transferred process due to the surface roughness of ZnO NRs from Fig. 3a. From the above mentioned result in Fig. 2a, the average diameter of ZnO NRs is about 100 nm. That is to say, the diameter ratio (γ) between PS sphere and ZnO NRs is close to 2, PS sphere arrays are very difficult to

Fig. 1 The schematic illustration of the fabrication processes of Au NSs/ZnO NRs structure: **a** bare ZnO NRs; **b** self-assembled polystyrene (PS) nanosphere monolayer on ZnO NRs using the modified dip-coating method; **c** the as-deposited PS Au shell structure; **d** Au NSs top-contacted ZnO NRs produced by annealing at 500 °C in air



form ordered structures. When the diameter ratio increases to 5, the homogeneity of PS arrays is perfect from Fig. 3b. With the further increasing of PS sphere diameter, γ is 7.5 and 10, respectively, we can observe that the surface roughness of ZnO NRs has no influence on PS sphere arrays in Fig. 3c, d.

After the samples annealed at 500 °C, the Au NSs form on the top of ZnO NRs. For the different PS sphere, the density and size of Au NSs appear obvious difference. The results show that the size of PS sphere is smaller, the density of Au NSs is sparser, and the size of Au NSs becomes bigger, as is shown in Fig. 4a–d. We assume that Au seeds on ZnO NRs

very easily grow up big Au NSs due to the small space between PS spheres, when the diameter of PS is 200 nm. At the same time, big Au NSs reunite and sinter bigger Au NSs. With increasing of the diameter of PS, the space of Au seeds on ZnO NRs becomes relatively sparse. So, Au NSs, which are formed by Au seeds, are difficult to aggregate again, when the diameter of PS spheres reaches 750 and 1000 nm.

To further investigate the structure properties of the Au NSs attached to ZnO NRs, XRD and EDS were carried out. The XRD patterns of the ZnO NRs, Au shell/ZnO NRs, and Au NSs/NRs structures are shown in Fig. 5. On all the samples, a

Fig. 2 SEM images of the bare ZnO NRs and Au NSs top-contacted ZnO NRs samples: **a** the bare ZnO NRs; **b** 1000 nm PS spheres coated with 20-nm Au film on ZnO NRs; **c** Au nanoshells arrays on ZnO NRs; **d** Au NSs top-contacted ZnO NRs

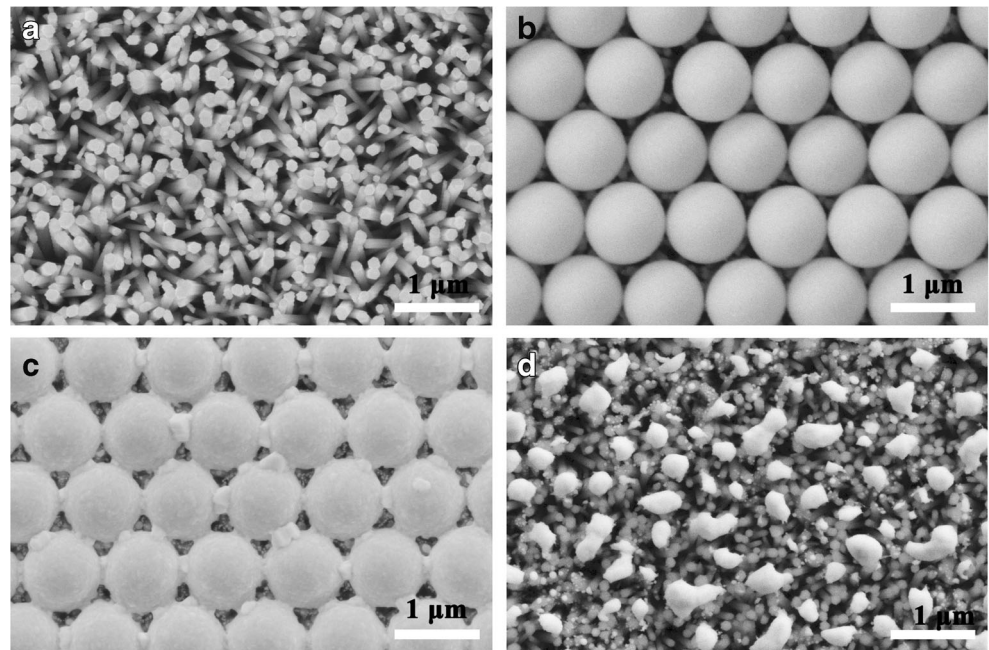
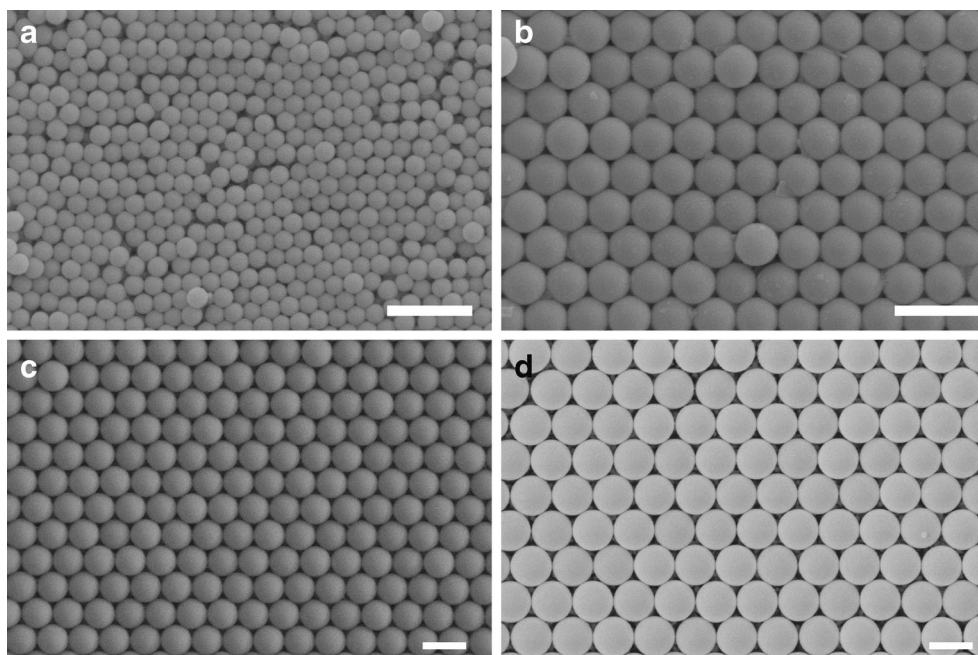


Fig. 3 SEM images of the different PS spheres on ZnO NRs samples: **a** 200 nm; **b** 500 nm; **c** 750 nm; **d** 1000 nm



dominant diffraction peak at 34.5° (2theta) was characterized as the wurtzite ZnO (002) diffraction, which indicates the preferential orientation along the wurtzite (002) direction in the ZnO NRs structure. It should be noted that the peak located at 38.1° (2theta), corresponding to the Au (111) plane, exhibits a stronger intensity in the Au NSs/NRs structures at high temperature than that in the Au shell/ZnO NRs sample at low temperature. The XRD patterns show that annealing temperature can affect the crystal structure. At the same time, EDS patterns can evidence Au content and ZnO crystal structure.

The more detailed information on morphologies and crystal structures of the Au NSs on the ZnO NRs composite was obtained from the TEM images and selected area electron diffraction (SAED) patterns. Figure 6a, c shows the low and high resolution TEM images of Au NSs on the ZnO NRs composite structures. It can be revealed that there are small Au nanoparticles left on the surface of the ZnO NRs structure. This can also be evidenced from the EDS patterns, as shown in Fig. 6c, d, where the spectra were collected from the regions of the Au NSs on the ZnO NRs.

Fig. 4 SEM images of the different PS spheres coated with 20-nm Au film on ZnO NRs samples annealed at 500°C : **a** 200 nm; **b** 500 nm; **c** 750 nm; **d** 1000 nm

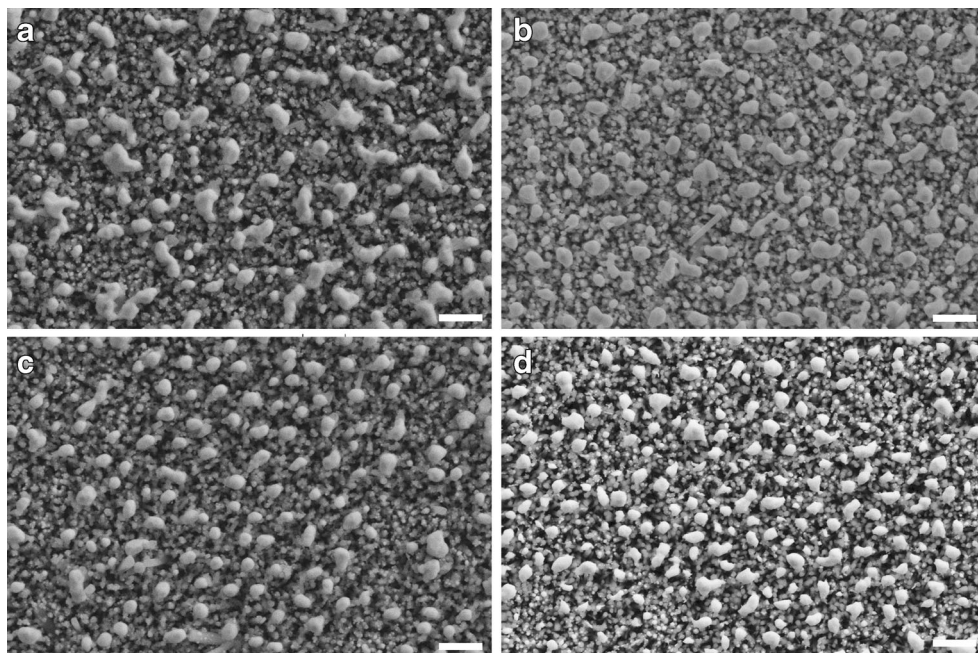
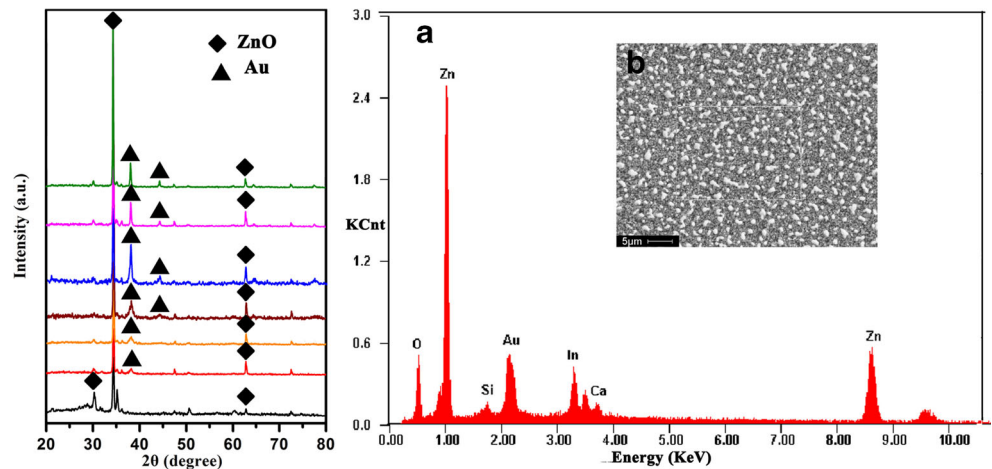


Fig. 5 XRD patterns and EDS of bare ZnO NRs, the Au shell/ZnO NRs, and Au NSs/ZnO NRs



PL Properties of Au NSs Top-contacted ZnO NRs with Different Density and Size

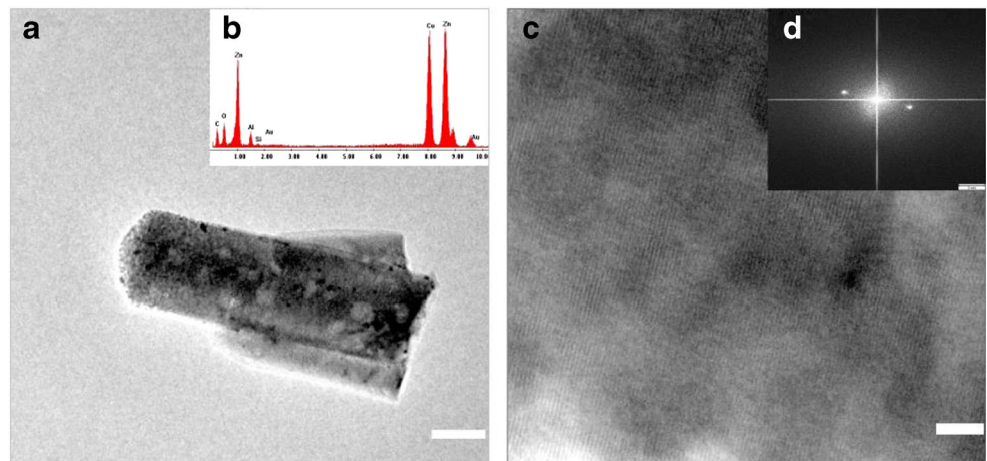
Figure 7 shows PL spectra of Au NSs top-contacted ZnO NRs with different density and size. PL spectra show that defect-related PL peak of the samples is at 620 nm and remained the same after annealing at 500 °C. However, luminous intensity gradually increased with decreasing of the size of Au NSs. It shows that the size and density of Au NSs are the key factors to influence the luminescence intensity of ZnO NRs. It has been reported that the surface plasmonic properties of Au nanoparticles usually red-shift with increasing of their size. The energy match between surface plasmons (SPs) from metal NPs and excitons in semiconductor materials is the key factor to achieve enhanced luminescence. The bigger Au NSs cannot effectively enhance the luminescence intensity of ZnO NRs due to the deviation between their resonance peaks and the defect-related

related peak of ZnO NRs. At the same time, the bigger Au NSs cannot provide more localized field energy for defect-related emission of ZnO NRs. So, luminous efficacy of Au NSs top-contacted ZnO NRs can be enhanced approximate five times with decreasing of the Au NSs size.

PL Properties of Au NSs Top-contacted ZnO NRs at Different Annealing Temperature

To compare the influence of annealing temperature on PL properties of bare ZnO NRs and the Au NSs on ZnO NRs, the samples of 1000 nm PS spheres on ZnO NRs annealed at 300, 400, and 500 °C, respectively. Figure 8 shows the room temperature PL spectra of ZnO NRs after annealing. For the bare ZnO NRs after annealing at 400 °C, a near band gap emission at around 378 nm and a broad and intense defect-related emission band centered at 560 nm are observed. After

Fig. 6 TEM images of **a** Au NSs on the ZnO NRs, **c** high resolution, **b** and **d** EDS patterns and the SAED pattern of the structure



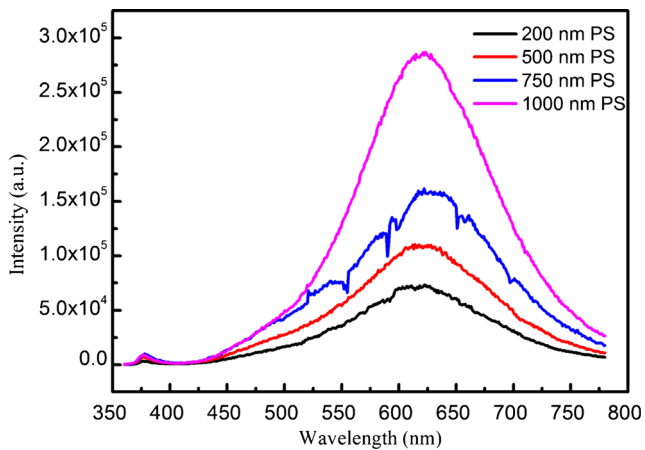


Fig. 7 Room temperature PL spectra of different Au NSs on ZnO NRs

annealing, it is found that the defect emission variably enhanced with annealing temperature. Moreover, the band edge emission intensity is suppressed for all samples. In addition, the defect-related emission band at 560 nm red-shifts to 620 nm. As shown, the increased defect emission and suppression of band edge emission are obviously related to the Au nanoparticles. In general, the broad defect emission is regarded to be related to surface defects such as oxygen vacancy (V_O) and/or Zn vacancy (V_{Zn}) and impurities [10]. However, another explanation is that surface plasmonic resonance effect brings about exciton-plasmon coupling between the ZnO NRs and Au NPs. In our experiment, annealing temperature is 300 °C, and Au shell arrays are large-scale coverage on the ZnO NRs. They suppress not only the band edge emission but also the defect-related emission. When NSs reached 200 nm nearby at 500 °C, the defect-related emission intensity of Au NSs on ZnO NRs is nearly twofold higher than that of bare ZnO

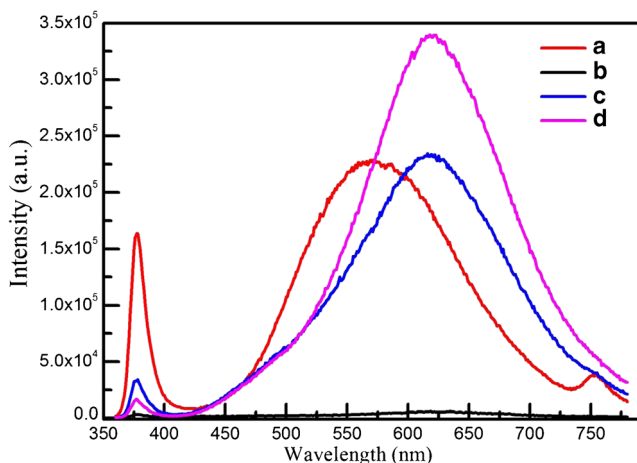


Fig. 8 Room temperature PL spectra of Au NSs on ZnO NRs at different annealing temperature

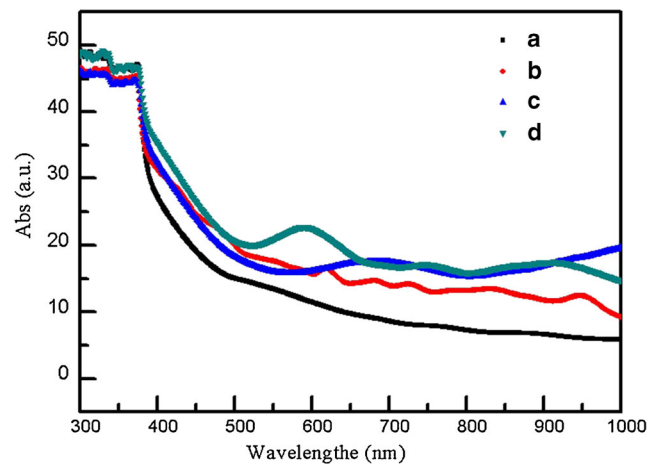


Fig. 9 Absorption spectra of the bare ZnO NRs and Au NSs top-contacted ZnO NRs

NRs. Considering the differences with or without the Au NSs decoration, the significant enhancement is from the strong interaction between the LSPs from Au NSs and the excitons in ZnO. However, the band edge emission enhancement is that the energy level of defect states matches with the Au nanoparticles Fermi level. Figure 9 shows the absorption spectra of bare ZnO NRs and various Au NSs on ZnO NRs. Comparing with bare ZnO NRs, Au NSs on ZnO NRs structures appear some obvious resonance peaks in the range of 550–700 nm. This means that LSPRs of Au NSs can provide more energy for electrons in the ZnO defect level. Hence, PL intensity of the defect-related emission of ZnO NRs is enhanced.

Conclusions

In summary, a simple technique based on a combination of NSL and thermal decomposition was proposed to fabricate Au NSs on the ZnO NRs. By controlling the annealing temperature and choosing the proper PS nanosphere template, top-contact Au NS on ZnO NRs arrays with a controllable size were prepared. The defect-related emission of ZnO NRs can be obviously enhanced by controlling Au NSs size. It is believed that these changes are mainly tuned by the coupling between spontaneous emission in ZnO NRs and SPs from the Au NSs. This kind of structure can also be easily integrated into other WBG semiconductor materials, such as GaN or SiC, to achieve luminescence enhancements and thus be potentially applied in optoelectronic devices.

Acknowledgments This research is supported by the National Natural Science Foundation of China (11074132), Natural Science Fund of Tianjin (11JCYBJC 06200), and the national training program (201410792019).

References

- Chang JA, Rhee JH, Im SH, Lee YH, Kim HJ, Seok SI, Nazeeruddin MK, Gratzel M (2010) High-performance nanostructured inorganic-organic heterojunction solar cells. *Nano Lett* 10(7):2609–2612
- Xu J, Yang X, Wang HK, Chen X, Luan CY, Xu ZX, Lu ZZ, Roy VAL, Zhang WJ, Lee CS (2011) Arrays of ZnO/ZnxCd1-xSe nanocables: Band gap engineering and photovoltaic applications. *Nano Lett* 11(10):4138–4143
- Park SH, Kim SH, Han SW (2007) Growth of homoepitaxial ZnO film on ZnO nanorods and light emitting diode applications. *Nanotechnology* 18(5):055608–055614
- Han JH, Liu ZF, Guo KY, Ya J, Zhao YF, Zhang XQ, Hong TT, Liu JQ (2014) High-efficiency AgInS₂-modified ZnO nanotube array photoelectrodes for all-solid-state hybrid solar cells. *ACS Appl Mater Interfaces* 6(19):17119–17125
- Chen H-Y, Liu K-W, Jiang M-M, Zhang Z-Z, Xie X-H, Wang D-K, Liu L, Li B-H, Zhao D-X, Shan C-X, Shen D-Z (2014) Tunable enhancement of exciton emission from MgZnO by hybridized quadrupole plasmons in Ag nanoparticle aggregation. *Appl Phys Lett* 104(9):091119–091123
- Zang Y, He X, Li J, Yin J, Li K, Yue C, Wu Z, Wu S, Kang J (2013) Band edge emission enhancement by quadrupole surface plasmon-exciton coupling using direct-contact Ag/ZnO nanospheres. *Nanoscale* 5(2):574–580
- Cheng CW, Sie EJ, Liu B, Huan CHA, Sum TC, Sun HD, Fan HJ (2010) Surface plasmon enhanced band edge luminescence of ZnO nanorods by capping Au nanoparticles. *Appl Phys Lett* 96(7):071107–071109
- Mahanti M, Basak D (2012) Highly enhanced UV emission due to surface plasmon resonance in Ag-ZnO nanorods. *Chem Phys Lett* 542:110–116
- Mahanti M, Basak D (2014) Enhanced photoluminescence in Ag@SiO₂ core-shell nanoparticles coated ZnO nanorods. *J Lumin* 154:535–540
- Lin HY, Cheng CL, Chou YY, Huang LL, Chen YF, Tsen KT (2006) Enhancement of band gap emission stimulated by defect loss. *Opt Express* 14(6):2372–2379
- Cheng P, Li D, Yuan Z, Chen P, Yang D (2008) Enhancement of ZnO light emission via coupling with localized surface plasmon of Ag island film. *Appl Phys Lett* 92(4):041119–041121
- Richters JP, Voss T, Kim DS, Scholz R, Zacharias M (2008) Enhanced surface-excitonic emission in ZnO/Al(2)O(3) core-shell nanowires. *Nanotechnology* 19(30):305202–305205
- Lin JM, Lin HY, Cheng CL, Chen YF (2006) Giant enhancement of bandgap emission of ZnO nanorods by platinum nanoparticles. *Nanotechnology* 17(17):4391–4394
- Sakano T, Tanaka Y, Nishimura R, Nedyalkov NN, Atanasov PA, Saiki T, Obara M (2008) Surface enhanced Raman scattering properties using Au-coated ZnO nanorods grown by two-step, off-axis pulsed laser deposition. *J Phys D Appl Phys* 41(23):235304–235309
- Chen ZH, Tang YB, Liu CP, Leung YH, Yuan GD, Chen LM, Wang YQ, Bello I, Zapien JA, Zhang WJ, Lee CS, Lee ST (2009) Vertically aligned ZnO nanorod arrays sensitized with gold nanoparticles for Schottky barrier photovoltaic cells. *J Phys Chem C* 113(30):13433–13437
- Jain PK, Lee KS, El-Sayed IH, El-Sayed MA (2006) Calculated absorption and scattering properties of gold nanoparticles of different size, shape, and composition: Applications in biological imaging and biomedicine. *J Phys Chem B* 110(14):7238–7248
- Link S, El-Sayed MA (1999) Size and temperature dependence of the plasmon absorption of colloidal gold nanoparticles. *J Phys Chem B* 103(21):4212–4217
- Lee K-S, El-Sayed MA (2006) Gold and silver nanoparticles in sensing and imaging: Sensitivity of plasmon response to size, shape, and metal composition. *J Phys Chem B* 110(39):19220–19225
- Liu Z, Ya J, E L (2010) Effects of substrates and seed layers on solution growing ZnO nanorods. *J Solid State Electrochem* 14(6):957–963
- Liu Z, E L, Ya J, Xin Y (2009) Growth of ZnO nanorods by aqueous solution method with electrodeposited ZnO seed layers. *Appl Surf Sci* 255(12):6415–6420
- Yan WG, Qi JW, Li ZB, Tian JG (2014) Fabrication and optical properties of Au-coated polystyrene nanosphere arrays with controlled gaps. *Plasmonics* 9(3):565–571
- Luo CL, Yan WG, Zhao J, Li Z-B, Tian J-G (2015) Surface plasmonic properties and fabrication of large area disordered and binary ordered au particle arrays. *Superlattice Microst* 85:92–100